

Research Report

Ex vivo Detection of Amyloid- β in Naturally Formed Oral Biofilm

Shalini Kanagasigam^a, Christopher von Ruhland^b, Richard Welbury^a and Sim K. Singhrao^{a,*}

^a*Brain and Behavior Centre, Faculty of Clinical and Biomedical Sciences, School of Dentistry, University of Central Lancashire, Preston, UK*

^b*Electron and Light Microscopy Facility, College of Biomedical and Life Sciences, Cardiff University, Wales, UK*

Received 21 September 2022

Accepted 18 November 2022

Pre-press 5 December 2022

Published 16 December 2022

Abstract.

Background: Oral infection has been implicated in the possible etiology of Alzheimer's disease.

Objective: To detect amyloid- β (A β) within microbial biofilms.

Methods: Freshly extracted teeth ($N=87$) with periodontal disease were separated into Group A ($N=11$), with primary root canal infection and Group B ($N=21$) with failed endodontic treatment identified by the presence of, gutta percha root filling. Biofilm characteristics were observed by scanning electron microscopy (SEM). Demineralized paraffin wax embedded tooth sections and mineralized calculus biofilm were immunostained with the anti-A β antibody. The gutta perchas were processed either for on-section acrylic resin tissue immunocolloidal gold silver staining (IGSS) using the anti-A β antibody or in Araldite resin for ultrastructure.

Results: SEM demonstrated calculus and gutta percha *in situ* harboring a polymicrobial biofilm featuring extracellular polymeric substance (EPS) and water channels. Immunohistochemistry on rehydrated paraffin wax tooth sections from Group A, demonstrated A β staining on external (calculus and plaque) and all intracanal infected regions. In Group B, the gutta percha biofilm IGSS gave an inconclusive result for A β . Transmission electron microscopy of selected teeth with infected intra-canal (Group A) and 20% of gutta percha biofilm (Group B) EPS contained electron dense fibrils of variable sizes, some of which were typical of human A β fibrils.

Conclusion: This study detected both soluble and insoluble A β fibrils within the EPS of periodontal and endodontic natural biofilm, strongly suggesting its role as an antimicrobial peptide in combatting local infection, with potential risk for cross-seeding into the brain for AD development.

Keywords: Amyloid- β fibrils, biofilm, extracellular polymeric substance, periodontal bacteria, root canal

INTRODUCTION

The sporadic form of Alzheimer's disease (AD) is a notoriously complicated disease without a confirmed etiology. This has led to the proposal of many hypotheses with one implicating infection of a

diverse cross-Kingdom microbial and multi-species of microorganisms including viruses, bacteria, fungi, and/or their virulence factors [1–9]. Supporting the infection hypothesis is the detection of considerably more bacterial DNA and bacterial outer membrane component lipopolysaccharide or LPS in AD brains than the age-matched non-AD subjects [4, 7, 9–12], which provides an appropriate explanation for the widespread inflammation in AD and the involvement of innate immunity [13–15].

*Correspondence to: Sim K. Singhrao, University of Central Lancashire, Preston, PR1 2HE, UK. E-mail: SKSinghrao@uclan.ac.uk.

Although Moir et al. [8] support a functional (microbicidal/antimicrobial/immune protection) role for amyloid- β (A β) in AD pathogenesis, the traditional view of insoluble A β in AD is considered pathogenic [16]. According to Dueholm and Nielsen [17] functional amyloids are a group of highly ordered fibrillar protein polymers which are characterized by a cross- β quaternary structure [18] and can self-assemble from their monomeric protein form. Histology of biofilms with amyloid specific dyes (Congo red, Thioflavin T/S), or amyloid conformation-specific antibodies has demonstrated that functional amyloids are widespread among naturally and otherwise formed microbial biofilms [19]. Within the biofilm context, these amyloids appear to play important roles in supporting biofilm ecosystems, and as such act as “functional” supports for the architecture of biofilms and for establishing the appropriate microbial communities. Examples of functional amyloids include microbial appendage proteins such as curli, pili, and fimbriae. These appendage proteins can be unique to each genus of bacteria, which under yet unknown physiological conditions, undergo conformational changes to form microbial A β fibrils [20–22].

Friedland [23] suggests a sinister role for the microbial amyloids because they may impose a potential risk for AD development through the phenomenon known as cross-seeding. This can happen by nucleation of proteins like, for example, prions in transmissible spongiform encephalopathies [24]. In support of the possible translocation of A β , Zeng et al. [25] have demonstrated the receptor for advanced glycation end products, which is upregulated in cerebral endothelial cells, following at least *P. gingivalis* infection. The theoretical basis of the A β cross-seeding as a risk for mental health proposed by Friedland [23] is also supported by the human microbiome project, which suggests that the gastrointestinal tract dysbiosis is associated with pathogenic mechanisms in AD [26]. Indeed, A β plaques have been observed in the submucosa of two AD patients [27] supporting the idea that AD brain pathophysiology may be initiated in the gastrointestinal tract.

A Taiwanese national insurance database study involving more than 200,000 cases of AD over 10 years, reported lower odds of dementia when procedures which removed the cause of infection were carried out such as endodontic treatment and limited extractions. Patients who had frequent periodontal emergencies and those who had more than 4 teeth extracted increased the odds of AD [28]. We

hypothesized that the root canal/periodontal disease infections may be a common denominator for the risk of developing AD. Endodontic disease is classified as primary or secondary microbial infections of the dental pulp, within the root canal system [29]. Most cases of root canal infection involve intra-radicular biofilm formation. If inadequately treated, this may lead to persisting or secondary infection [30]. Periodontal disease, better known as ‘periodontitis’, involves chronic inflammation and infection of the tooth supporting tissues, caused by a polymicrobial dysbiosis associated with biofilm on the external root surface in the form of calculus and plaque [31, 32]. As the pulp and the periodontium communicate via multiple anatomical pathways, an endodontic lesion can affect the periodontium and conversely, a periodontal lesion can instigate pulpal disease [33, 34]. If left untreated, both endodontic and periodontal disease can result in pain, spreading infection, and eventual tooth loss.

Kobayashi et al. [35] reported that microorganisms common to root canal infections are also found in periodontal disease lesions called pockets [36]. These include *Eubacterium* and *Fusobacterium* species, *Porphyromonas gingivalis*, *Prevotella intermedia*, *Peptostreptococcus*, *Capnocytophaga*, *Actinomyces*, and *Streptococcus* genera of bacteria. Interestingly, *A. naseslundii* and *P. gingivalis* have been identified in AD postmortem brain tissue by next generation sequencing methodologies [7, 10, 11] and by immunohistochemistry [37, 38]. There is already strong evidence to link AD with periodontitis, as well as the role of its keystone pathogen, *P. gingivalis* as a significant risk factor for cognitive decline [4, 9, 39–42].

Given that all human cells express the *amyloid beta protein precursor* (A β PP) gene, the gingival tissue (epithelial cell barrier) is shown to be rich in soluble A β [9], it may be plausible to suggest that the upregulated A β PP and/or soluble A β is constantly released as an antimicrobial peptide in response to oral biofilms [43]. The *Enterococcus* and *Streptococcus* species of bacteria express curli fibers [19, 44]. If bacterial curli fibers are known for their human equivalent A β fibrils, then it is plausible to suggest that an endodontic biofilm in the human host could exhibit A β /A β -like deposits in the extracellular polymeric substance (EPS), which would be visible by high resolution ultrastructure using transmission electron microscopy (TEM) [19]. The rationale for this study comes from reports that bacteria harbor several proteins, for example, curli on their surface membranes that under appropriate pathophysiological

cal conditions assemble as functional amyloid fibers within their biofilm EPS component [19]. Alternatively, if the infection is within the host tissue, then potentially the human A β could be secreted in response as an antimicrobial peptide defense mechanism. Thus, there is a potential for finding both human and microbial amyloid. The implication is that the human and microbial A β protein in the oral cavity may be transported to the brain by the receptor for advanced glycation end products [25] and thereby cross-seed A β in the brain and become a risk factor for AD. This *ex vivo* pilot study is aimed at detecting the presence of host/bacterial amyloids within naturally formed endodontic biofilm in freshly extracted diseased human teeth.

MATERIALS AND METHODS

Ethical approval and NHS general dental practice recruitment

Following approval from the integrated research application system (IRAS study number 249743), Health Research Authority (HRA) and health and Care Research Wales (HCRW) approval from Research Ethics Committee (REC) reference number 19/NI/0019, ethical approval from the University of Central Lancashire (UCLan) was obtained for the proposed research project (UCLan STEM reference number 1001).

Once all the necessary ethical approvals were granted researchers proceeded to recruit NHS general dental practices in the North-West region of England, United Kingdom. Researchers asked dental practices to recruit consenting patients in the study who were cognitively healthy adults between the age of 50–90 years undergoing dental extraction due to dental health reasons only, and who voluntarily consented to donating their extracted tooth. Baseline demographics asked for was their age, gender and if they also suffered from type II diabetes (Table 1).

Table 1

Baseline demographics asked for age, gender and if they also suffered from type II diabetes

Gender	Consenting participants	Average age	Type II diabetes
Males	41/87 = 47%	2,539/41 = 62 y	5/41 = 12%
Females	46/87 = 53%	3,016/46 = 66 y	9/46 = 20%

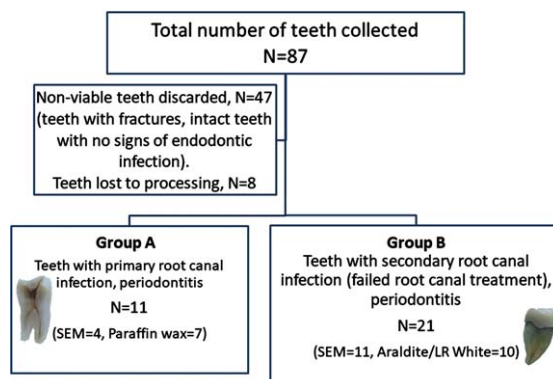


Fig. 1. Flowchart of the study. A flowchart of the study shows the total number of freshly extracted teeth collected from NHS dental practices ($N = 87$), of which 47 teeth were found to be non-viable due to stated reasons and 8 teeth were lost due to processing. The study groups were divided into teeth with primary root canal infection and periodontitis (Group A, $N = 11$) and teeth with secondary root canal infection (failed root canal treatment) and periodontitis (Group B, $N = 21$). In Group A, 4 teeth were processed for SEM imaging and 7 teeth were processed for paraffin wax embedding. In Group B, 11 teeth were processed for SEM imaging and 10 teeth along with gutta-percha were divided up for LR White resin and Araldite.

Specimen collection

Eighty-seven extracted teeth were placed in a pot of 70% ethanol bearing the IRAS study number (Fig. 1) by the dental surgeon in charge of the patient on the day of the extraction. Once the pot was nearly full, the dental practice alerted the researchers for its collection. In the laboratory, the teeth were logged on the HTA register using LIMs software with a bar coding system called 'Samples version 2.8' (Ziath Ltd., <https://ziath.com>) and then fixed in 10% neutral buffered formalin (Sigma-Aldrich) for 24 h at 4°C. All human teeth were stored in the human tissue designated room as per the Human Tissue Act (2004) UK regulations.

Scanning electron microscopy (SEM) for external root calculus and gutta percha biofilm

Out of the 87 teeth, 4 teeth (Group A) were examined by SEM for high resolution morphological examination of the external (root calculus) and internal (root canal) biofilm ($N = 4$). These teeth belonged to Group A for determining calculus biofilm characteristics such as EPS and water channels. In addition, gutta percha *in-situ* from Group B ($N = 11$) were examined under the SEM following further fixation in 2.5% glutaraldehyde diluted in 0.01 M phosphate

buffered saline (PBS, pH 7.4) for up to 3 h at 4°C followed by 1 prolonged wash in excess PBS overnight at 4°C. Next day, the specimens were post fixed in 2% aqueous osmium tetroxide solution for 2 h at room temperature in a fume hood. The teeth were dehydrated in graded alcohols from 70% ethanol to absolute alcohol 3 times for 30 min each. The fully dehydrated teeth were further dried free of alcohol in a bench top glass vacuum desiccator for up to 24 h and sputter coated with gold using the Emitech K550X sputter coater [45]. Examination and imaging of the specimens was performed using the FEI Quanta 200 SEM.

Collection of scraped root calculus

Out of the remaining 83 teeth, 5 teeth were selected for removal of calculus deposits using a sterile scalpel blade and collected into prelabelled tubes containing PBS for paraffin wax embedding. These undamaged teeth were then returned to the collection of remaining teeth ($N=83$ final) for demineralization.

Demineralization of teeth

The teeth ($N=83$) were demineralized in 10% ethylenediaminetetraacetic acid or EDTA (pH 7.4) with 0.07% glycerol for approximately 1–3 months depending on the type of tooth (incisors, premolars, and molars). Upon adequate demineralization the teeth were cut in the plane of the gutta percha with the intact biofilm for examination using light microscopy and TEM.

Paraffin wax embedding

Scraped root calculus and intracanal biofilm in teeth with primary root canal infection

The scraped root calculus deposits (Group A, $N=5$) and teeth (Group A, $N=7$) with primary root canal infection lesions were dehydrated in graded ethanol (70, 80, 100%) and cleared in 3 changes of xylene and embedded in paraffin wax (Sigma-Aldrich) as per routine pathology laboratory methodology.

Resin embedding

Araldite CY212

The intact biofilm on the gutta percha (Group B, $N=10$), were cut into 3 mm² pieces and further divided for dedicated TEM and for immunocolloidal

gold silver staining (IGSS) techniques. For dedicated TEM, primary root canal infected teeth and the selected biofilms *in situ* on the gutta percha were fixed in 2.5% glutaraldehyde and post fixed in 2% aqueous osmium tetroxide (Agar Scientific UK). The specimens were fully dehydrated and the standard dedicated TEM protocols for resin infiltration and embedding in Araldite CY212 containing specimen identity labels was followed as published elsewhere [46].

LR White resin

The intact biofilm on the 3 mm² pieces of gutta percha (Group B, $N=10$), undergoing LR White resin embedding, were partially dehydrated in 70% ethanol, and infiltrated in a mixture of 70% ethanol:LR White resin in the ratio of 1:3 for 1 h. Further infiltration (3 times for 1 h each) followed in pure LR White resin [47]. The specimen blocks were embedded in fresh cold LR White (Agar scientific UK) to which manufacturer's accelerator was added in the ratio of 1.5 µL/mL in prelabelled polypropylene Beem[®] capsules using the cold catalytic method [48].

Positive controls for on-section immunocolloidal gold silver staining

AD transgenic Tg2576 mouse brains with the Swedish mutation ($N=3$) previously obtained from Prof. Roxane O. Carare, Faculty of Medicine, University of Southampton, UK to act as positive controls for A β plaques in the Bahar et al. [49] study was in our possession as paraffin embedded tissue blocks. The University of Central Lancashire, UK, having previously approved our application to the AWERB committee for use of the Tg2576 mice brains (RE/17/06). From 1/3 blocks, a paraffin wax embedded Tg2576 (positive control) mouse brain containing A β plaques was chosen, and the brain tissue was excised, dewaxed in xylene followed by alcohol exchanges. The mouse brain tissue was rehydrated to 0.01 M phosphate buffered saline (PBS, pH 7.4). From here the Tg2576 mouse brain tissue and the gutta percha biofilm were processed and embedded in LR White resin using the previously published procedure [47].

Sectioning

Paraffin wax blocks

Sections were prepared from two sources of paraffin wax embedded tissue blocks: calculus (min-

eralized form) and Group A primary root canal infected teeth (demineralized) with caries. The tissue blocks were sectioned (4 μm thickness) using the Leitz 1512 rotary microtome (Marshall Scientific) and collected on 0.1% gelatin coated glass microscope slides.

Resin blocks

All tissues embedded in resin blocks were sectioned using glass knives on the Leica Reichert Ultracut E microtome (Leica Biosystems). Semi-thin sections (below 1 μm thickness) were collected on glass slides for Toluidine blue staining. The ultra-thin sections (80–100 nm thickness) were collected onto 300 mesh naked nickel grids (Agar scientific UK) for examination under the TEM.

Light microscopy

Gram's stain

The primary root canal infected teeth and the calculus sections from paraffin wax were subjected to Gram's stain adopted from a published method with tissue sections [49]. Briefly, rehydrated paraffin wax tissue sections were subjected to crystal violet (PL.8000) solution (Pro-lab Diagnostics, UK) for 1 min and flooded with Lugol's iodine (PL.7052) solution for 1 min with washes in between. Gram differentiator (PL.7006/25) was applied to the slide drop wise, until no more color was released. Following further washings in distilled water, the slide was counter-stained with Safranin O (PL.7012) for 30–60 seconds and washed prior to air drying and mounting under a glass coverslip using Gurr's DPX. The slides were examined under a Nikon Eclipse E200 Microscope and imaged using the DS-L2 v.441 Software (Nikon, UK).

Immunohistochemistry

Sections were dewaxed in xylene and washed in alcohol changes (3 x for 5 min each) prior to quenching the endogenous peroxidase activity using 0.03% H_2O_2 in methanol for 30 min.

Antigen retrieval

The rehydrated sections were exposed to neat formic acid (Sigma-Aldrich, UK) for 10 min in the fume hood, at room temperature. The sections were washed thoroughly in water before equilibrating them in PBS for 5 min.

Non-specific antibody binding

The non-specific antibody binding to tissue sections was blocked by treatment of sections for 30 min in blocking solution containing 0.01% normal horse serum in PBS, pH 7.0 (Vectastain kit, PK 4001).

Antibody omission negative controls

Block solution alone was included as primary antibody omission control in each experiment.

Positive control

Serendipitously, a 3mm² inflamed gingival tissue attached to an extracted tooth was identified (by histology) and upon immunostaining this section was found useful to act as a positive control for immunostaining with anti-A β antibody.

Mouse anti-A β antibody

Where appropriate, the negative and positive control sections alongside of the test sections were incubated overnight at 4°C, in mouse anti-A β antibody (clone 6e10, BioLegend) diluted 1/200 in block (see above). Next day, the sections were washed free of the primary antibody (3 x for 5 min each) in PBS before re-incubating the sections in the secondary detection antibody from the Vectastain ABC HRP kit PK- 4002 (Vector Laboratories), for mouse IgG according to the suppliers' instructions. The detection was completed using the DAB peroxidase kit (SK-4100), again according to the suppliers' instructions. The sections were lightly counterstained with 0.1% Light Green (C.I. 42095, Sigma-Aldrich) [51], rapidly dehydrated in alcohol and cleared in xylene before mounting under glass coverslips in Gurr's neutral mounting medium (Thermo Scientific). Examination of sections and image capture was carried out as above for the Gram's stain.

Toluidine blue staining: All semi-thin resin sections on glass slides

A drop of filtered 0.5% Toluidine blue in 0.5% borax was placed for about 20 s (LR White) and 60 s (Araldite CY212) onto the semi-thin section on microscope glass slide placed on a hotplate set to 65°C. The excess stain was immediately washed off under the tap water and the section was fully dried (on the hotplate), before mounting under a glass coverslip in Gurr's DPX mounting medium (Fisher Scientific).

Immunocolloidal gold silver staining

LR White resin embedded Tg2576 mouse brain and gutta percha biofilm

No antigen retrieval was carried out with formic acid.

Antibody omission negative controls

PBS/BSA alone was included as primary antibody omission controls in each experiment.

Positive control

Tg2576 mouse brain tissue sections from a suitable LR White resin embedded block were used as a positive control with anti-A β antibody.

Mouse anti-A β antibody

To determine an appropriate antibody titer for subsequent immunohistochemical staining of the biofilm specimens, positive control mouse brain sections were equilibrated for 10 min in 20 mM PBS pH 7.4 containing 0.6% bovine serum albumin (PBS/BSA) followed by 1 h in anti-A β antibody (clone 6e10) diluted in PBS/BSA to a range of dilutions (1/100, 1/200, 1/500, 1/1000, 1/2000, 1/5000, and 1/10,000). PBS/BSA alone was included as primary antibody omission controls. Sections were washed for 2 x 1 min in PBS/BSA and 1 min in 20 mM tris buffer pH 7.4 containing 0.6% bovine serum albumin (TBS/BSA) followed by 1 h in anti-mouse IgG conjugated to 10 nm colloidal gold (Sigma-Aldrich). Sections were thoroughly washed in distilled water and allowed to air dry. Immunocolloidal gold staining was visualized by subjecting the sections to photochemical intensification solutions (A and B) prepared in-house according to reference [52] for 20 min. Following thorough washings in distilled water, sections were lightly counterstained with 0.1% Light green as for immunochemistry of paraffin wax sections. The sections were fully air dried and mounted under a coverslip in Gurr's neutral mounting medium. A dilution of 1/2000 was chosen and applied to Tg2576 brain tissue sections (positive controls) alongside of the test gutta percha biofilm sections as described above.

Araldite embedded biofilm sections staining for ultrastructure

The grids were fully immersed for 20 min in filtered, 2% aqueous uranyl acetate solution (Taab Ltd.) on a sheet of dental wax and thoroughly washed in distilled water (3 x 2 min each). The grids were then

treated for 5 min in Reynolds [53] lead citrate solution followed by further washings in distilled water (3 x 2 min each) and air dried. The grids were examined in a Hitachi HT7800 TEM (Hitachi High Tech Ltd., UK) at 100 kV and images were captured with Radius software (EMSIS GmbH, Germany).

RESULTS

A total of 87 teeth were collected following all ethical approvals from cognitively healthy, voluntarily consenting adults between the age of 50–90 years from the North-West of England, UK who at the time were undergoing dental extraction for dental health reasons only. Non-viable teeth ($N=47$) were discarded as they demonstrated either fractures or were without signs of endodontic infection. Teeth ($N=8$) were lost during demineralization and paraffin wax processing steps. Teeth ($N=32$) were placed into groups A and B (Fig. 1) according to primary or secondary root canal infection and were examined for the presence of A β .

The baseline demographics collected were age, gender, and if they suffered from type II diabetes (Table 1). The youngest donor was 51 years age and the eldest was 82 years with majority being in their mid-fifties to mid-sixties. The gender was generally well balanced (males = 47%; females = 53%) with slightly higher proportion of females (66%) than men (62%). More females were suffering from type II diabetes (20%) than males (12%) Table 1. Teeth were separated into three categories namely, vital teeth, teeth with primary endodontic infection, and teeth with secondary endodontic infection (failed root canal treated teeth) (Fig. 1).

SEM: Biofilm characteristics

SEM employed for high resolution morphological examination of the root calculus from the external tooth root surface of a primary endodontic infection (Fig. 2A, thick black arrow). Under the SEM, the calculus deposits were visible harboring a polymicrobial biofilm with cocci (Co) and rod (Ro) shaped bacteria embedded within the matrix (Fig. 2B). On higher magnification the EPS was observed as a smooth structure (Fig. 2C, EPS) harboring mainly cocci (Co) shaped bacteria and only a few rod-shaped bacteria. Multiple water channels (Fig. 2C, white arrows) were clearly visible throughout the EPS.

Extracted human teeth ($N=11$, demineralized) with a history of failed root canal treatment were

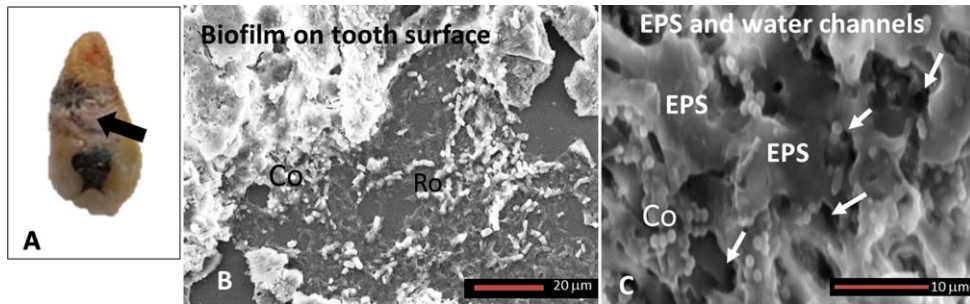


Fig. 2. Calculus on a tooth's external surface for biofilm characteristics. A) Macroscopic image of an extracted tooth (black arrow) to show calculus and plaque deposits on the external root surface. B) SEM images of the calculus deposits from the external tooth root surface shown in A revealed a polymicrobial biofilm composed mainly of cocci (Co) and rod (Ro) shaped bacteria. C) The biofilm shows extracellular polymeric substance (EPS) with smooth appearance on which cocci (Co) shaped bacteria are clearly visible with the occasional rod (Ro) shaped bacterium. Smooth EPS demonstrated an abundance of water channels with variable openings as indicated by white arrows. Magnification as per micron bar.

sectioned longitudinally so that the gutta percha remained *in situ* (Fig. 3A). SEM imaging confirmed the presence of early biofilm establishing along the gutta percha with discrete colonies of various morphotypes of bacteria (Fig. 3C, D). Figure 3C and 3D are magnified areas demarcated by boxes in Fig. 3B (from a typical early biofilm) and the arrows point to each image corresponding to the box.

Light microscopy

Gram's stain characteristics

An overview of a tooth as a line drawing shows the basic anatomy and orientation of a diseased tooth (Fig. 4A) as a reference to the tooth sections shown following Gram's stain. The extracted human root section demonstrated clusters (thick blue arrows) of Gram-positive bacteria amongst the Gram-variable stained microbes on the external root surface, on the caries lesion (Fig. 4B), and internally to the infected tooth canal and adjacent root dentine showing Gram-positive bacteria (Fig 4C). Double headed arrow (Fig. 4C) indicates the coronal to apical orientation of the root canal space and adjacent root dentine with respect to Fig. 4A. The root calculus (Fig. 4D, E) also demonstrated a mixture of filamentous Gram-positive and non-filamentous Gram-variable bacteria embedded within the ECM.

Immunohistochemistry: paraffin wax

The inflamed gingival tissue used as a positive control demonstrated strong immunostaining in epithelial cells with the anti-A β antibody (clone 6e10), which at the light microscopy level appeared to be in its soluble form (Fig. 5A). All primary

root canal infections associated with caries demonstrated immunostaining with the anti-A β antibody, which was more strongly localized to clumps of bacteria (Fig. 5B blue filled arrow) that were of a Gram-positive characteristic (as shown in Fig. 4B) compared to those that were Gram-variable (Fig. 5B). All primary root canal infected teeth associated with caries lesions within the intracanal biofilm (Fig. 5B oval shape and the square with broken lines) immunostained with the anti-A β antibody. The negative control (primary antibody omitted) section taken from the mineralized root calculus scraps remained free of any immunostaining (Fig. 5C). The mineralized root calculus alongside the positive and negative control tissue sections demonstrated immunostaining localized to the presumed biofilm bacteria or its EPS (Fig. 5D).

On-section immunocolloidal gold silver staining of LR White resin embedded gutta percha biofilm

The Tg2576 mouse brain sections used as a positive control demonstrated strong immunostaining of the insoluble A β deposits with the anti-A β antibody (clone 6e10, Fig. 6A). The negative control whereby the primary antibody was omitted on a tissue section taken from Tg2576 brain remained free of any immunostaining (Fig. 6B). The gutta perchas with thick naturally formed biofilm as presented in Fig. 6C were examined by embedding them in resin media. The gutta perchas (Gp) and their associated biofilm (Bf) are shown by demarcation with broken lines (Fig. 6D–F), which often drifted away from the gutta percha in stained preparations. Negative control sections (Fig. 6D) remained free of specific immunostaining. The semi-serial gutta percha (Gp) and its

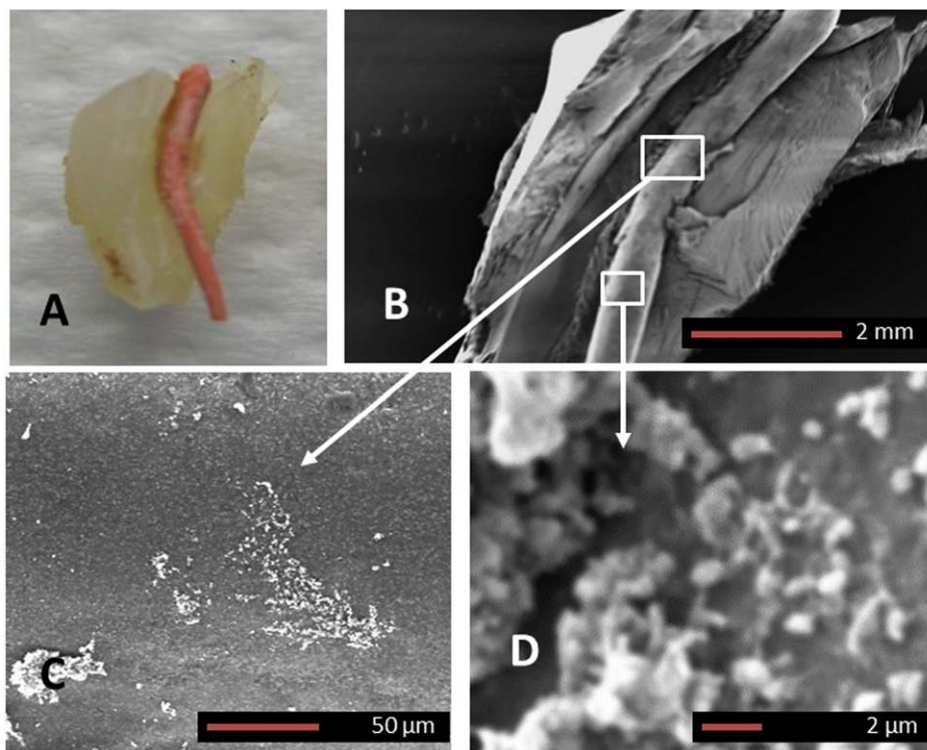


Fig. 3. Gutta percha biofilm SEM. A) Macroscopic image of an extracted human tooth with a history of failed root canal treatment which was sectioned longitudinally exposing the intact gutta percha. B) SEM image of the gutta percha within the root canal. Higher magnifications of the white squares in B, demarcated by arrows are shown in C and D. Panels C and D confirm the presence of an early biofilm formation on the gutta percha (Magnifications as per micron bar).

associated biofilm (Bf) did not show any significant A β immunostaining in all gutta percha biofilms examined although only two gutta percha biofilms (anti-A β 1, and 2) are shown as examples (Fig. 6E, F).

Semi-thin Araldite sections

Toluidine blue staining

The biofilm bacteria (Bf) within the gutta-percha (Gp) associated biofilm appeared to be well preserved and were of various morphotypes (cocci, rods and filamentous, Fig. 7A, B). The gutta percha material remained relatively intact after processing in resin media and appeared greenish blue to greyish with black spots in it (Fig. 7B) following Toluidine blue staining.

Ultrastructure

Infected root canal tooth

The caries tooth sections with internal root canal infection under the TEM demonstrated that the denti-

nal canals were laden with bacteria taking up a variety of rounded and elongated shapes (Fig. 8A). Freshly infected dentinal tubules (Fig. 8A circles with broken lines) demonstrated abundant collagen surrounding the dentinal tubules. The longer-term infected tubules appeared to have degraded bacteria within them and the host tissue around the tubules also appeared degraded (Fig. 8, insert). On closer examination of the degraded tissue from the boxed area in Fig. 8A, insert under the TEM revealed the presence of fibrils resembling insoluble A β (Fig. 8B, black arrows).

Gutta percha biofilm

The ultrastructure of the biofilm confirmed the variety of morphotypes of the biofilm bacteria that were seen in light microscopy Toluidine blue preparations (Fig. 7A). Based on the thick electron dense wall, both Gram-positive and Gram-variable bacteria were observed (Fig. 9A). Higher magnification images clearly demonstrated EPS (Fig. 9B–F) in between bacterial cells. The internal content of a bacterium appeared to contain “virus-like” particles (Fig. 9B circle, and 9C, insert). Examination of the

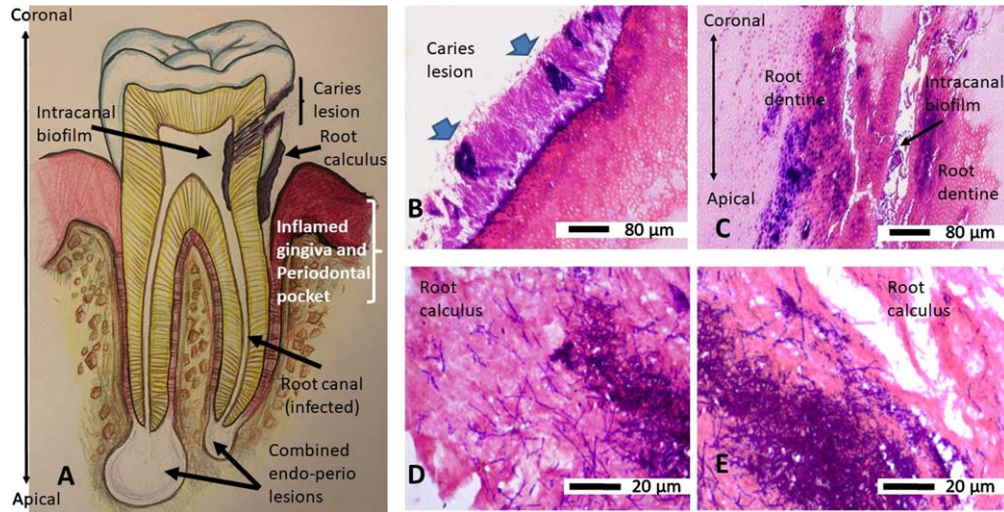


Fig. 4. An overview and orientation of a diseased tooth (line drawing) and Gram's stain characteristics of the infecting bacteria. Panel A is a line drawing of a tooth as a map for the tissues and their orientation in Gram-stained images. B) Demineralized, paraffin wax embedded, rehydrated section of a tooth from a primary root canal infection (Group A) showing a carious lesion with clusters of Gram-positive (blue) bacteria (blue arrows) and Gram-variable bacteria on the external surface. C) Same tissue section as in B shows the infection had spread internally within the canal and dentinal tubules of the tooth. Double headed arrow indicates the coronal to apical orientation of the root canal space and adjacent root dentine with respect to panel A. D, E) Paraffin wax embedded, rehydrated sections of scraped root calculus shows both Gram-positive (blue) bacteria intermingled with filamentous and non-filamentous Gram-variable bacteria.

EPS at greater magnification from Fig. 9D, areas within the larger oval shape and yellow star demonstrated some short electron dense fibrils within the electron lucent amorphous matrix. Further examination of the gutta percha biofilm (Fig. 9G) showed more fibrils (area demarcated with a line and two arrows to show few fibrils) were clearly different in morphology (longer) to those seen in Fig. 9E and 9F. Continued searching of the specimen under the TEM demonstrated more very fine long fibrils (Fig. 9H, black arrows) which appeared very similar to the fibrils observed in Fig. 8B, presumed host A β .

DISCUSSION

Epidemiological studies have demonstrated an association between chronic periodontal disease and AD [54, 55]. These studies correlate with clinical research which measured circulating antibodies to two periodontal bacteria (*F. nucleatum* and *P. intermedia*) which were linked to cognitive deficit 10 years later. An interventional study measured inflammatory markers in AD patients before and after dental treatment linking periodontal bacteria to cognitive deficit [56]. Other researchers reported the correlation between periodontal disease with serum levels of A β [57] and higher amyloid load in the brain in older, mentally healthy patients with periodontal

disease [58]. The latter two studies implicated the role of peripheral inflammation, possibly due to periodontal disease, causing higher A β build up in these patients. Apart from inflammation it is also plausible that gingipains secreted by *P. gingivalis* itself can cleave the A β PP at the β - and δ -secretase sites, which may further add to the pools of A β in the brain [43] preclinically as well as once AD is manifested.

The design of the present study was influenced by Lin et al. [28] where endodontic treatment and limited extractions of grossly carious teeth were identified as factors which appeared to lower the odds of developing AD. Lin et al. [28] study also evaluated the association with major comorbidities and found that diabetes was proportionately more prevalent in dementia patients. A similar effect was seen in patients who had frequent periodontal emergencies and those who had more than 4 teeth extracted [28].

The tooth pulp and periodontium are closely connected via anatomical and pathological pathways. Dental caries can cause pulpal infection, which if left untreated can progress to pulpal necrosis. This eventually leads to apical periodontal tissue breakdown (known as apical periodontitis). Similarly, the etiology and pathobiology of periodontitis involves bacterial infection with pathological changes affecting the coronal periodontal tissues as shown in Fig. 4A. Untreated endodontic disease has been

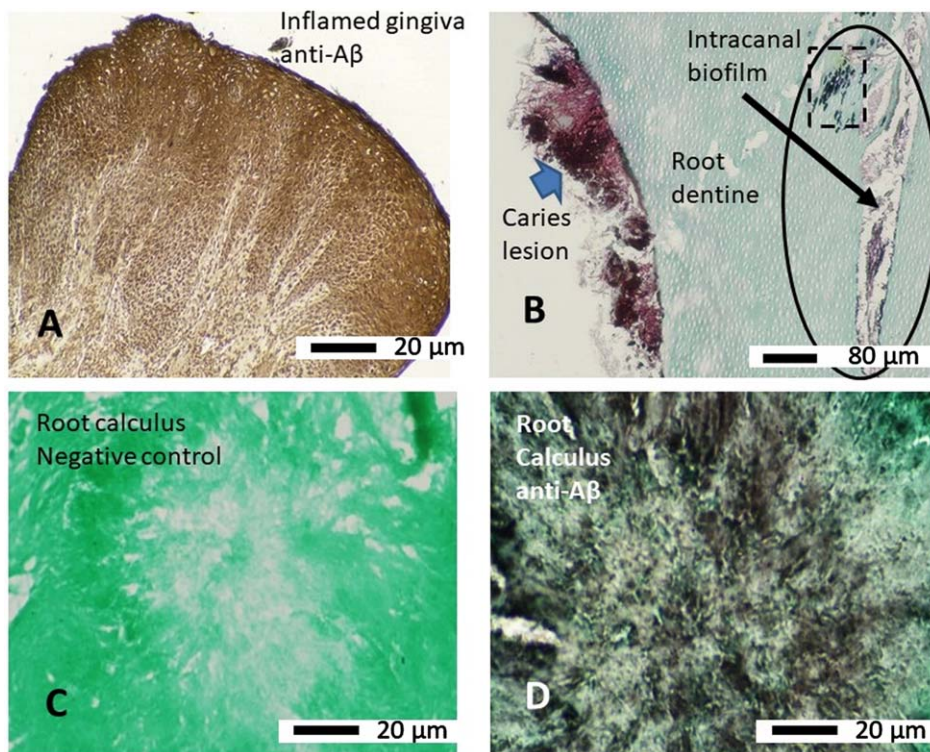


Fig. 5. Immunohistochemistry (paraffin wax sections) of microbial biofilm with anti-A β (clone 6e10) antibody. A) Human inflamed gingival tissue which was attached to an extracted tooth used as a positive control for immunostaining with anti-A β antibody. B) A tooth section from a primary root canal infection associated with a carious lesion (external to the tooth) showing more intense staining with anti-A β antibody on clusters of Gram-positive bacteria (blue arrow) whilst the Gram-variable clusters of bacteria are also positive with the antibody. The intracanal biofilm (oval shape and arrow) and intra-tubular biofilm (square with broken line, within the oval shape) also demonstrated immunostaining with the anti-A β antibody. C) Negative control (omission of primary antibody) of root calculus shows there is no non-specific antibody binding. D) An adjacent section of root calculus shown in C immunostained with anti-A β antibody shows brown staining of soluble A β around the microbes within the biofilm.

considered a local modifying risk factor for the progression of periodontal disease [59–61] and possibly for AD [29]. Molecular studies have identified *P. gingivalis*, *Parvimonas micra*, and *Tannerella forsythia* as the main microbes in both endodontic and periodontal diseases. Clustering of oral bacteria at the genus level included *Streptococcus*, *Parvimonas*, *Prevotella*, *Actinomyces*, *Fusobacterium*, *Treponema*, and *Filifactor* [62, 63]. Rocas et al. [64] detected significantly more *Enterococcus faecalis* in cases of persistent infections associated with cases of failed endodontic treatment [64] implying the possibility of finding microbial functional A β in our gutta percha biofilm. The sampling carried out in the present study comprised of extracted teeth which had combined periodontal and endodontic disease, from patients with an average age of 64 years of which 22% of the donors were type II diabetics. The specimens included teeth with primary endodontic infections as well as teeth with secondary infections

(with persistent disease) in order to fully represent the natural clinical biofilm, present in patients' oral environments.

The present study employed morphological and immunohistochemical analyses with the aim to detect insoluble A β . Initially, morphological imaging was explored for the presence of biofilm, microorganisms and EPS with water channels, characteristics which define a true biofilm. Immunohistochemistry was used to detect A β ; however, in the absence of antibodies to microbial functional amyloid such as anti-curli antibodies, a high-resolution ultrastructure approach was adopted for visualizing insoluble A β as per previous studies [19]. Insoluble A β or A β -like deposits were observed via TEM imaging of the biofilm both within the root canals of infected teeth and in the gutta percha biofilm. However, the biofilm attached to the internal and external surfaces of teeth in Group A displayed strong immunostaining to the anti-A β antibody. This indicated that teeth

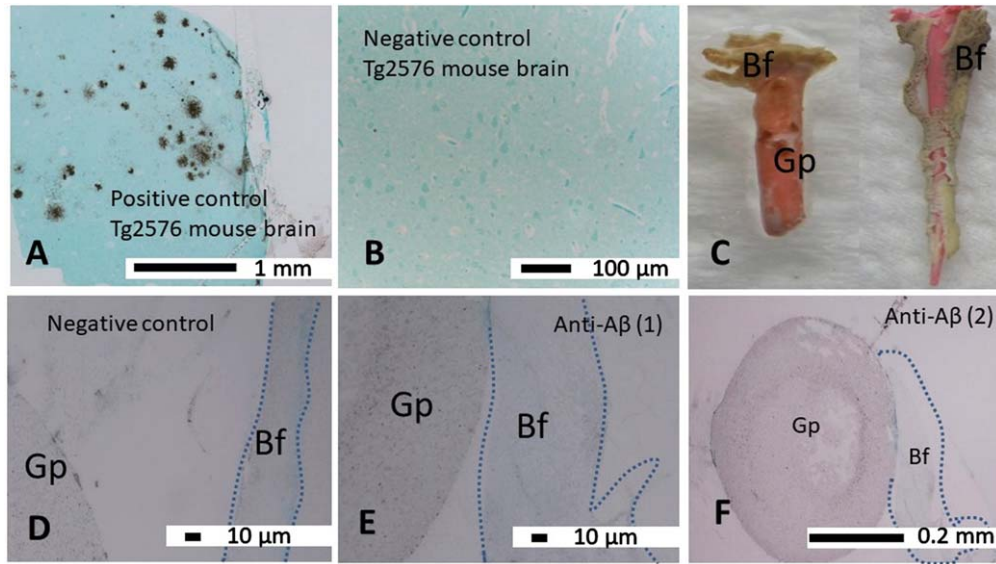


Fig. 6. Immunocolloidal gold silver staining (IGSS) of LR White resin embedded gutta percha biofilm sections. A) The Tg2576 mouse brain sections used as a positive control demonstrated insoluble A β deposits with the anti-A β antibody (clone 6e10). B) The negative control whereby the primary antibody was omitted on a tissue section taken from Tg2576 brain remained free of any non-specific immunostaining. C) Macroscopic image of two gutta perchas (Gp) in their native color orange and pink, freshly removed from demineralized teeth are covered by biofilm within the sealer cement coating (cream-grey colored). D–F) The gutta percha (Gp) and its associated biofilm (Bf) are demarcated by broken lines. D) The negative control section remained free of specific immunostaining. E, F) The semi-serial sections of the gutta percha (Gp) and its associated biofilm (Bf) did not show significant amounts of A β in gutta percha associated biofilms examined at the light microscopy level with anti-A β (1) and (2) are shown as examples.

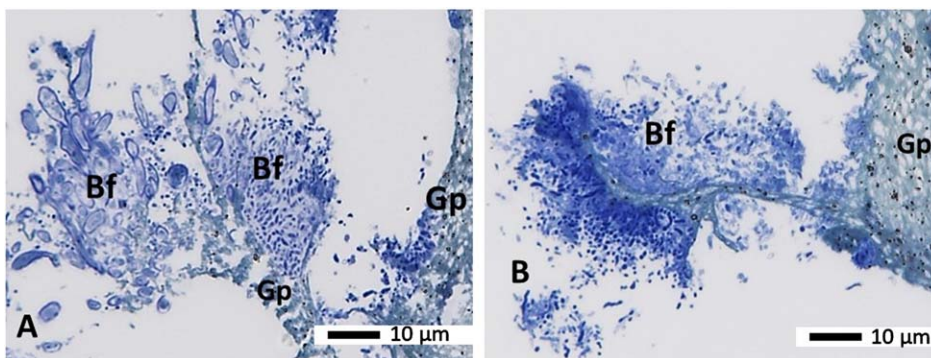


Fig. 7. Semithin sections from a gutta percha from a failed root treatment (secondary endodontic infection Group B) embedded in Araldite resin. Panels A and B show semi-thin sections stained with the morphology stain Toluidine blue showing the biofilm (Bf) on the gutta percha (Gp). A variety of microbes (stained blue) can be seen growing on and slightly away from the gutta percha (Gp), which has a green/blue/greyish shade with black dots in it. Magnification as per micron bar.

with primary endodontic infection which still harbor live pulpal tissue may have released soluble A β in response to the infection. The innate immune response is essential in protecting dental hard and soft tissues from infectious insults such as carious lesions as well as periodontal dysbiotic biofilms [65].

Both caries and periodontal disease can instigate pulpal infection and inflammation. Once activated, the innate immune system triggers the diffu-

sion of inflammatory mediators, pro-inflammatory cytokines, chemokines, and bacterial toxins into the periapical region, resulting in apical bone resorption [66]. This is comparable to the destruction of alveolar bone seen in periodontal disease whereby the invasion of the periodontium by pathogens can cause an excessive innate immune response. Soluble antimicrobial proteins provide a network of signals to coordinate the immediate molecular and cellular

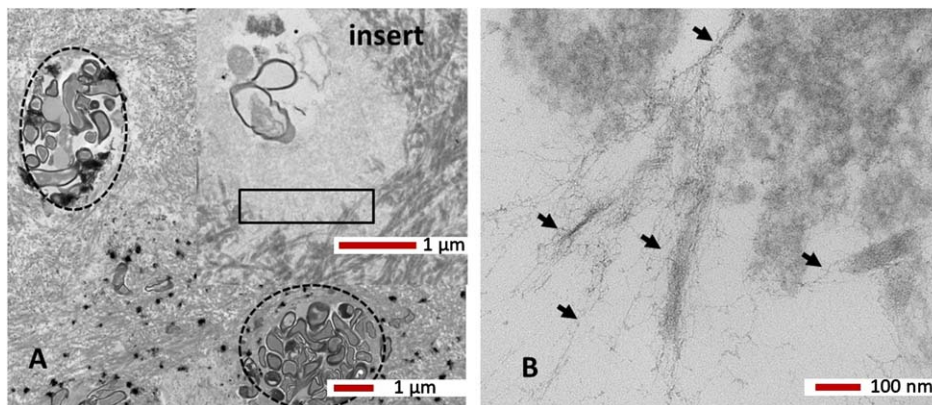


Fig. 8. TEM High resolution ultrastructure. A tooth section from a primary root canal infection associated with caries (see Fig. 5B, area in the oval shape) shows dentinal tubules laden with bacteria (broken line circles). A higher magnification of a dentinal tubule with fewer but degraded bacteria (insert in A) and degraded collagen demonstrated insoluble fibrils (in areas within the rectangle), which are shown in B) at higher magnification. The fine fibrils appeared very similar to the host A β (black arrows). Magnification as per micron bar.

reaction to infection [65]. Based on the antimicrobial protection hypothesis [8], A β can be part of the innate immune response as opposed to a purely pathological outcome [67]. Fani et al. [67] reported that higher levels of phenotypical serum markers of innate immunity were associated with higher plasma levels of A β in a population-based study. In the present study, in Group B, (which consisted of extracted teeth with periodontitis and failed endodontic treatment), the root canal system and extracted gutta percha biofilm all demonstrated soluble and insoluble A β . This may be explained by the fact that all tooth surrounding soft

tissues (gingivae, periodontal ligament, pulpal cells) are actively secreting soluble A β to keep the innate immune response ticking over within the root canal system.

The endodontic tooth harbors a microbiome of its own in which a consortium of multispecies of microbes reside inside the pulp that are difficult to eliminate. In this study, the gutta percha biofilm in which some host tissues (for example, collagen fibrils) were seen (confirmed by ultrastructure), and demonstrated, what appears ultra-structurally to be insoluble A β . In a previous study Kanagasingam et al.

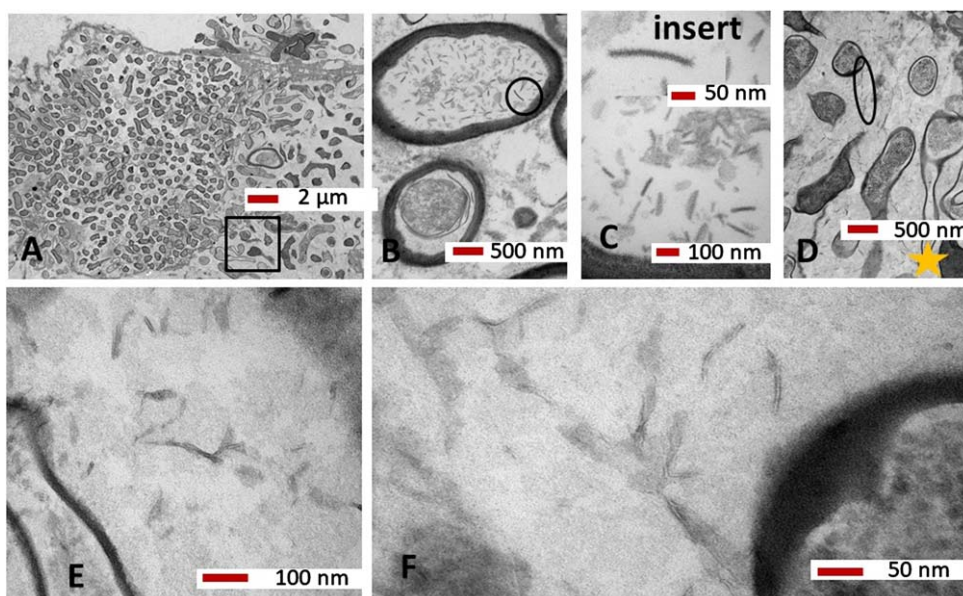


Fig. 9. (Continued)

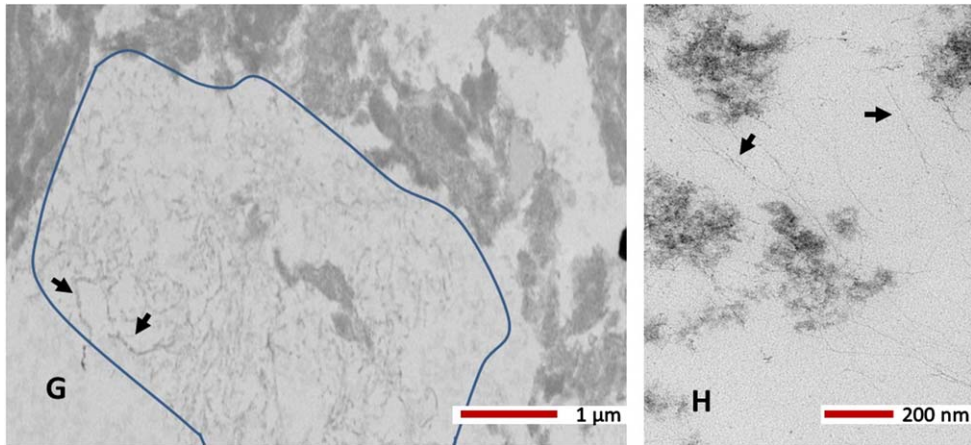


Fig. 9. A–F) Ultrastructure of a gutta percha biofilm embedded in Araldite resin. Panel A shows a variety of morphotypes of the biofilm bacteria. Panel B shows an internal content of a bacterium to contain virus-like particles (circle). C) The insert shows a higher region (from B, circle) for clarity on the virus-like particle. D) On the basis of the thick wall, both Gram-positive and Gram-negative bacteria were observed alongside the EPS (circle and oval shapes). E) Area demarcated by the yellow star from panel D. F) Area within the larger oval shape from panel D at higher magnification with some short electron dense fibrils within the EPS. G, H) More fibrils. Further examination of the gutta percha biofilm in panel G shows more fibrils (area demarcated with a line and two arrows show the fibrils) which were clearly different in morphology to those seen in panels E and F. H) Even more very fine fibrils (black arrows) were observed which appeared very similar to the host A β observed in Fig. 8B. Magnification as per micron bar.

[43] demonstrated very similar fibrils from A β synthetic peptide (used as a control) and from *in vitro* *P. gingivalis* cultures. This suggests the gutta percha biofilm harbors both human A β and microbial A β like short fibrils and suggests necrotic human tissue getting caught up within the gutta percha biofilm thereby gives rise to the human A β . The root canal infections are typically caused by Gram-positive facultative anaerobic bacteria of genera such as *Enterococci*, *Streptococci*, *Lactobacilli*, *Actinomyces*, and *Candida* [68–71]. Of these, *Enterococci* genus of bacteria typically harbor curli, pili, and fimbriae, which the literature links to microbial amyloids once they have undergone appropriate pathophysiological changes to assemble as functional amyloid fibers [19].

As mentioned before, Moir et al. [8] support a functional (microbicidal/antimicrobial/immune protection) role for A β and the present study does support this viewpoint. However, the fact that host soft tissues which are likely to have been degraded by the proteases of the biofilm microbes also appear to be surrounded by A β fibrils as though they too are being attacked. An alternative explanation would be that if A β is a true antimicrobial peptide then this could be due to the non-specific nature of the innate immune defense mechanism. This also supports the traditional view of insoluble A β being pathogenic [16].

Although the pathological form of prion proteins has not been detected in dental pulp tissue, there is a theoretical risk of cross infection in individuals with Creutzfeldt-Jakob disease via endodontic instruments which contact pulpal neurovascular tissue during root canal treatment. Studies have shown that the prion-protein resists conventional sterilization methods and may transfer these proteins from infectious Creutzfeldt-Jakob disease patients [72, 73]. The pathogenic isoform of prions has a three-dimensional conformation with a higher β -sheet content which exhibits decreased solubility, leading to the deposition of insoluble fibrils in A β plaques. When cross-seeding occurs involving the central nervous system, prions can cause spongiform degeneration. This was considered sufficient justification for national organizations, including the Disease Control and Prevention and World Health Organization to restrict endodontic instruments to single use as a precautionary measure [74–76]. As far as the authors are aware, this is the first time that potentially pathogenic insoluble A β fibers have been detected within root canals of endodontically and periodontally infected teeth. The clinical significance of these findings raises concerns over the extent of dissemination of the A β from the oral sources can enter the central nervous system in a similar manner to prions, thereby instigating and/or contributing to AD neurodegeneration.

Conclusions

The present study has been valuable as a pilot study to understand the microbial biofilm A β from naturally formed oral heterogenous consortium of bacterial communities. The major strength being that they were naturally formed in the human host, which include the host-related parameters including age, local environmental factors, similar immune status, and lifestyle, such as diet and oral health condition.

The host appears to have responded to the infection by releasing A β as an innate response in group A tooth biofilms and to the gutta percha associated biofilm. Overall, this study detected insoluble A β within the periodontal and endodontic natural biofilm formation parameters. Clinical significance of the present study is that endodontic teeth can harbor multi-Kingdom species of microbes including viruses, and bacteria. These microbes can give rise to insoluble A β experimentally, not dissimilar to the mechanism with which prions deposit insoluble fibrils in A β plaques. Like prions, insoluble A β will remain a risk for being cross seeded to the brain and for the plausible development of AD later in life. Further research is required to clarify the extent of such a risk and the mechanism by which A β could translocate from the mouth to the brain.

Limitations and strengths of the study

Limitations of this study are a small N number. Absence of at least a pan antibody to microbial functional amyloids such as curli protein. Each extracted tooth could not be traced back to the donor, for example, if it came from a patient who suffered from type II diabetes or otherwise a healthy individual.

The strengths of this study are that the biofilms investigated were from human donors formed in a relatively senior age group from both males and females under patient based environmental/behavioral conditions for the true evaluation of insoluble A β .

Future studies

Future studies should include additional investigations such as DNA sequencing to identify the predominant bacteria, specifically from the *Enterococci* genus which typically harbor bacterial amyloid precursors curli, pili, and fimbriae that are said to form the elements of microbial A β under appropriate pathophysiological conditions. Alternatively test for at least one microbial functional amyloid such as curli

protein. Specific immunocolloidal A β labeling of the fine filaments (assumed A β) should be performed at the ultrastructure level to confirm their identity for host A β and/or for microbial curli protein contribution. Investigations should include larger sample size and assess potential correlations with patients' comorbidities.

ACKNOWLEDGMENTS

The authors would like to express their sincere gratitude to the participating dental practices in the North-West of England, UK, and the tooth donors without whom the study would not have been completed. We also like to thank the various ethics committees for their guidance in the application process and granting approval for the study to begin in 2018.

FUNDING

SK and SKS acknowledge funding for this project from PreViser in 2017 from the Oral and Dental Research Trust.

CONFLICT OF INTEREST

The authors have no conflict of interest to report.

REFERENCES

- [1] Fischer O (1910) Die presbyoprene demenz, deren anatomische grundlage und klinische abgrenzung. *Z Gesamte Neurol Psychiatr* **3**, 371–471.
- [2] Miklossy J (1993) Alzheimer's disease a spirochetosis. *Neuroreport* **4**, 841-848.
- [3] Balin BJ, Little CS, Hammond CJ, Appelt DM, Whittum-Hudson JA, Gérard HC, Hudson AP (2008) Chlamydophila pneumoniae and the etiology of late-onset Alzheimer's disease. *J Alzheimers Dis* **13**, 371-380.
- [4] Poole S, Singhrao SK, Kesavalu L, Curtis MA, Crean StJ (2013) Determining the presence of periodontopathic virulence factors in short-term post-mortem Alzheimer's disease brain tissue. *J Alzheimers Dis* **36**, 665-677.
- [5] Zhan X, Stamova B, Jin LW, DeCarli C, Phinney B, Sharp FR (2016). Gram-negative bacterial molecules associate with Alzheimer disease pathology. *Neurology* **87**, 2324-2332.
- [6] Itzhaki RF, Lathe R, Balin BJ, Ball MJ, Bearer EL, Braak H, Bullido MJ, Carter C, Clerici M, Cosby SL, Del Tredici K, Field H, Fulop T, Grassi C, Griffin WS, Haas J, Hudson AP, Kamer AR, Kell DB, Licastro F, Letenneur L, Lövheim H, Mancuso R, Miklossy J, Oth C, Palamara AT, Perry G, Preston C, Pretorius E, Strandberg T, Tabet N, Taylor-Robinson SD, Whittum-Hudson JA (2016) Microbes and Alzheimer's disease. *J Alzheimers Dis* **51**, 979-984.

- [7] Alonso R, Pisa D, Aguado B, Carrasco L (2017) Identification of fungal species in brain tissue from Alzheimer's disease by next-generation sequencing. *J Alzheimers Dis* **58**, 55-67.
- [8] Moir RD, Lathe R, Tanzi RE (2018) The antimicrobial protection hypothesis of Alzheimer's disease. *Alzheimers Dement* **14**, 1602-1614.
- [9] Dominy SS, Lynch C, Ermini F, Benedyk M, Marczyk A, Konradi A, Nguyen M, Haditsch U, Raha D, Griffin C, Holsinger LJ, Arastu-Kapur S, Kaba S, Lee A, Ryder MI, Potempa B, Mydel P, Hellvard A, Adamowicz K, Hasturk H, Walker GD, Reynolds EC, Faull RLM, Curtis MA, Draganow M, Potempa J (2019) Porphyromonas gingivalis in Alzheimer's disease brains: Evidence for disease causation and treatment with small-molecule inhibitors. *Sci Adv* **5**, eaau3333.
- [10] Emery DC, Shoemark DK, Batstone TE, Waterfall CM, Coghill JA, Cerajewska TL, Davies M, West NX, Allen SJ (2017) 16S rRNA next generation sequencing analysis shows bacteria in Alzheimer's post-mortem brain. *Front Aging Neurosci* **9**, 195.
- [11] Siddiqui H, Eribe E, Singhrao S, Olsen I (2019) High throughput sequencing detect gingivitis and periodontal oral bacteria in Alzheimer's disease autopsy brains. *Neurosci Res* **1**. doi.org/10.35702/nrj.10003
- [12] Zhan X, Stamova B, Sharp FR (2018) Lipopolysaccharide associates with amyloid plaques, neurons and oligodendrocytes in Alzheimer's disease brain: A review. *Front Aging Neurosci* **22**, 42.
- [13] Akiyama H, Barger S, Barnum S, Bradt B, Bauer J, Cole GM, Cooper NR, Eikelenboom P, Emmerling M, Fiebich BL, Finch CE, Frautschy S, Griffin WS, Hampel H, Hull M, Landreth G, Lue L, Mrak R, Mackenzie IR, McGeer PL, O'Banion MK, Pachter J, Pasinetti G, Plata-Salaman C, Rogers J, Rydel R, Shen Y, Streit W, Strohmeyer R, Tooyoma I, Van Muiswinkel FL, Veerhuis R, Walker D, Webster S, Wegrzyniak B, Wenk G, Wyss-Coray T (2000) Inflammation and Alzheimer's disease. *Neurobiol Aging* **21**, 383-421.
- [14] McGeer PL, McGeer EG (2002) Local neuroinflammation and the progression of Alzheimer's disease. *J NeuroVirol* **8**, 529-538.
- [15] Heneka MT, Golenbock DT, Latz E (2015) Innate immunity in Alzheimer's disease. *Nat Immunol* **16**, 229-236.
- [16] Alzheimer A (1907) Über eine eigenartige Erkrankung der Hirnrinde, *Allgemeine Z Psychiatr Psychisch-gerichtliche Med* **64**, 146-148.
- [17] Dueholm MS, Nielsen PH (2017) Amyloids – a neglected child of the slime. In *The Perfect Slime, Microbial Extracellular Polymeric Substances (EPS)*, Flemming HC, Neu TR, Wingender J, eds. IWA Publishing, London, UK, pp. 113-134.
- [18] Fandrich M (2007) On the structural definition of amyloid fibrils and other polypeptide aggregates. *Cell Mol Life Sci* **64**, 2066-2078.
- [19] Chapman MR, Robinson LS, Pinkner JS, Roth R, Heuser J, Hammar M, Normark S, Hultgren SJ (2002) Role of Escherichia coli curli operons in directing amyloid fiber formation. *Science* **295**, 851-855.
- [20] Sunde M, Serpell LC, Bartlam M, Fraser PE, Pepys MB, Blake CC (1997) Common core structure of amyloid fibrils by synchrotron x-ray diffraction. *J Mol Biol* **273**, 729-739.
- [21] Jimenez J, Guijarro JI, Orlova E, Zurdo J, Dobson CM, Sunde M, Saibil HR (1999) Cry-electron microscopy structure of an SH3 amyloid fibril and model of the molecular packing. *EMBO J* **18**, 815-821.
- [22] Nelson R, Sawaya MR, Balbirnie M, Madsen AO, Riekel C, Grothe R, Eisenberg D (2005) Structure of the cross- β spine of amyloid-like fibrils. *Nature* **435**, 773-778.
- [23] Friedland RP (2015) Mechanisms of molecular mimicry involving the microbiota in neurodegeneration. *J Alzheimers Dis* **45**, 349-362.
- [24] Eisenberg DS, Sawaya MR (2017) Structural studies of amyloid proteins at the molecular level. *Annu Rev Biochem* **86**, 69-95.
- [25] Zeng F, Liu Y, Huang W, Qing H, Kadowaki T, Kashiwazaki H, Ni J, Wu Z (2021) Receptor for advanced glycation end products up-regulation in cerebral endothelial cells mediates cerebrovascular-related amyloid β accumulation after *Porphyromonas gingivalis* infection. *J Neurochem* **158**, 724-736.
- [26] Minter MR, Zhang C, Leone V, Ringus DL, Zhang X, Oyler-Castrillo P, Much MW, Liao F, Ward JF, Holtzman DM, Chang EB, Tanzi RE, Sisodia SS (2016) Antibiotic-induced perturbations in gut microbial diversity influences neuro-inflammation and amyloidosis in a murine model of Alzheimer's disease. *Sci Rep* **6**, 30028.
- [27] Joachim CL, Mori H, Selkoe DJ (1989) Amyloid beta-protein deposition in tissues other than brain in Alzheimer's disease. *Nature* **341**, 226-230.
- [28] Lin JW, Chang CH, Caffrey JL (2020) Examining the association between oral health status and dementia: A nationwide nested case-controlled study. *Exp Biol Med (Maywood)* **245**, 231-244.
- [29] Siqueira JF Jr, Rôças IN (2009) Diversity of endodontic microbiota revisited. *J Dent Res* **88**, 969-981.
- [30] Siqueira JF Jr (2001) Strategies to treat infected root canals. *J Calif Dent Assoc* **29**, 825-837.
- [31] Socransky SS, Haffajee AD, Cugini MA, Smith C, Kent RL Jr (1998) Microbial complexes in subgingival plaque. *J Clin Periodontol* **25**, 134-144.
- [32] Hajishengallis G, Kajikawa T, Hajishengallis E, Maekawa T, Reis ES, Mastellos DC, Yancopoulou D, Hasturk H, Lambris JD (2019) Complement-dependent mechanisms and interventions in periodontal disease. *Front Immunol* **10**, 406.
- [33] Simon JHS, Glick DH, Frank AL (1972) The relationship of endodontic-periodontic lesions. *J Periodontol* **43**, 202-208.
- [34] Herrera D, Retamal-Valdes B, Alonso B, Feres M (2018) Acute periodontal lesions (periodontal abscesses and necrotizing periodontal diseases) and endo-periodontal lesions. *J Periodontol* **89(Suppl 1)**, S85-S102.
- [35] Kobayashi T, Hayashi A, Yoshikawa R, Okuda K, Hara K (1990) The microbial flora from root canals and periodontal pockets of non-vital teeth associated with advanced periodontitis. *Int Endod J* **23**, 100-106.
- [36] Caton JG, Armitage G, Berglundh T, Chapple ILC, Jepson S, Kornman KS, Mealey BL, Papapanou PN, Sanz M, Tonetti MS (2018) A new classification scheme for periodontal and peri-implant diseases and conditions - Introduction and key changes from the 1999 classification. *J Clin Periodontol* **45 Suppl 20**, S1-S8.
- [37] Howard J, Pilkington GJ (1992) Fibronectin staining detects micro-organisms in aged and Alzheimer's disease brain. *Neuroreport* **3**, 615-618.
- [38] Pisa D, Alonso R, Rábano A, Rodal I, Carrasco L (2015) Different brain regions are infected with fungi in Alzheimer's disease. *Sci Rep* **5**, 15015.

- [39] Hajishengallis G, Darveau RP, Curtis MA (2012) The keystone-pathogen hypothesis. *Nat Rev Microbiol* **10**, 717-725.
- [40] Ilievski V, Zuchowska PK, Green SJ, Toth PT, Ragozzino ME, Le K (2018) Chronic oral application of a periodontal pathogen results in brain inflammation, neurodegeneration and amyloid beta production in wild type mice. *PLoS One* **13**, e0204941.
- [41] Kanagasigam S, Chukkappalli SS, Welbury R, Singhrao SK (2020) *Porphyromonas gingivalis* is a strong risk factor for Alzheimer's disease. *J Alzheimers Dis Rep* **4**, 501-511.
- [42] Ryder M, Detke M, Sabbagh M, Bolger J, Hennings D, Skljarevski V, Kapur S, Raha D, Ermini F, Nguyen M, Haditsch U, Perry K, Ritch K, Hendrix S, Sam Dickson S, Hasturk H, Horine S, Mallinckrodt C, Holsinger LJ, Lynch C, Dominy S (2022) A role for *P. gingivalis* in Alzheimer's disease: Evidence from the GAIN Study. An abstract for the data presented at the 4th international Conference on *P. gingivalis* in Louisville, Kentucky.
- [43] Kanagasigam S, von Ruhland C, Welbury R, Chukkappalli SS, Singhrao SK (2022) *Porphyromonas gingivalis* conditioned medium induces amyloidogenic processing of the amyloid precursor protein upon *in vitro* infection of SH-SY5Y cells. *J Alzheimers Dis Rep* **6**, 577-587.
- [44] Taglialegna A, Matilla-Cuenca L, Dorado-Morales P, Navarro S, Ventura S, Garnett JA, Lasa I, Valle J (2020) The biofilm-associated surface protein Esp of *Enterococcus faecalis* forms amyloid-like fibers. *NPJ Biofilms Microbiomes* **6**. doi.org/10.1038/s41522-020-0125-2
- [45] Lal S, Pearce M, Achilles-Day UEM, Day JG, Morton LHG, Crean S, Singhrao SK (2017) Developing an ecologically relevant heterogeneous biofilm model for dental-unit waterlines. *Biofouling* **33**, 75-87.
- [46] Dillon A, Singhrao SK, Achilles-Day UE, Pearce M, Glyn Morton LG, Crean S (2014) *Vermamoeba vermiformis* does not propagate *Legionella pneumophila* subsp. *pascullei* in a simulated laboratory dental-unit waterline system. *Int Biodeterioration Biodegrad* **90**, 1-7.
- [47] Singhrao S, Cole G, Henderson WJ, Newman GR (1990) LR White embedding allows a multi-method approach to the analysis of brain tissue from patients with Alzheimer's disease. *J Histochem* **22**, 257-268.
- [48] Newman GR, Hobot JA (1987) Modern acrylics for post-embedding immunostaining techniques. *J Histochem Cytochem* **35**, 971-981.
- [49] Becerra SC, Roy DC, Sanchez CJ, Christy RJ, Burmeister DM (2016) An optimized staining technique for the detection of Gram positive and Gram negative bacteria within tissue. *BMC Res Notes* **9**. doi: 10.1186/s13104-016-1902-0
- [50] Bahar B, Kanagasigam S, Tambuwala MM, Aljabali AAA, Dillon SA, Doaei S, Welbury R, Chukkappalli SS, Singhrao SK (2021) *Porphyromonas gingivalis* (W83) infection induces Alzheimer's disease like pathophysiology in obese and diabetic mice. *J Alzheimers Dis* **82**, 1259-1275.
- [51] Goldner J (1938) A modification of the Masson trichrome technique for routine laboratory purposes. *Am J Pathol* **14**, 237-243.
- [52] Newman GR, Jasani B (1998) Silver development in microscopy and bioanalysis: A new versatile formulation for modern needs. *Histochem J* **30**, 635-645.
- [53] Reynolds ES (1963) The use of lead citrate at high pH as an electron opaque stain in the electron microscopy. *J Cell Biol* **17**, 208-212.
- [54] Sparks Stein P, Steffen MJ, Smith C, Jicha G, Ebersole JL, Abner E, Dawson D 3rd (2012) Serum antibodies to periodontal pathogens are a risk factor for Alzheimer's disease. *Alzheimers Dement* **8**, 196-203.
- [55] Chen CK, Wu YT, Chang YC (2017) Association between chronic periodontitis and the risk of Alzheimer's disease: A retrospective, population-based matched-cohort study. *Alzheimers Res Ther* **9**, 56.
- [56] Ide M, Harris M, Stevens A, Sussams R, Hopkins V, Culliford D, Fuller J, Ibbett P, Raybould R, Thomas R, Punter U, Teeling J, Perry VH, Holmes C (2016) Periodontitis and cognitive decline in Alzheimer's disease. *PLoS One* **11**, e0151081.
- [57] Gil-Montoya JA, Barrios R, Santana S (2017) Association between periodontitis and amyloid β peptide in elderly people with and without cognitive impairment. *J Periodontol* **88**, 1051-1058.
- [58] Kamer AR, Pirraglia E, Tsui W, Rusinek H, Vallabhajosula S, Mosconi L, Yi L, McHugh P, Craig RG, Svetcov S, Linker R, Shi C, Glodzik L, Williams S, Corby P, Saxena D, de Leon MJ (2015) Periodontal disease associates with higher brain amyloid load in normal elderly. *Neurobiol Aging* **36**, 627-633.
- [59] Gomes BPFA, Berber VB, Kokaras AS, Chen T, Paster BJ (2015) Microbiomes of endodontic-periodontal lesions before and after chemomechanical preparation. *J Endod* **41**, 1975-1984.
- [60] Ehnevid H, Jansson L, Lindskog S, Blomlöf L (1993) Periodontal healing in teeth with periapical lesions. A clinical retrospective study. *J Clin Periodontol* **20**, 254-258.
- [61] Zehnder M, Gold SI, Hasselgren G (2002) Pathologic interactions in pulpal and periodontal tissues. *J Clin Periodontol* **29**, 663-671.
- [62] Rufp S, Kannengießer S, Merte K, Pfister W, Sigusch B, Eschrich K (2000) Comparison of profiles of key periodontal pathogens in periodontium and endodontium. *Dent Traumatol* **16**, 269-275.
- [63] Li H, Guan R, Sun J, Hou B (2014) Bacteria community study of combined periodontal-endodontic lesions using denaturing gradient gel electrophoresis and sequencing analysis. *J Periodontol* **85**, 1442-1449.
- [64] Rôças IN, Siqueira JF Jr, Santos KR (2004) Association of *Enterococcus faecalis* with different forms of periradicular diseases. *J Endod* **30**, 315-320.
- [65] Meyle J, Dommisch H, Groeger S, Giacaman RA, Costalonga M, Herzberg M (2017) The innate host response in caries and periodontitis. *J Clin Periodontol* **44**, 1215-1225.
- [66] Stashenko P, Teles R, D'Souza R (1998) Periapical inflammatory responses and their modulation. *Crit Rev Oral Biol Med* **9**, 498-521.
- [67] Fani L, Ahmad S, Ikram MK, Ghanbari M, Ikram MA (2021) Immunity and amyloid beta, total tau and neurofilament light chain: Findings from a community-based cohort study. *Alzheimers Dement* **17**, 446-456.
- [68] Sundqvist G (1994) Taxonomy, ecology, and pathogenicity of the root canal flora. *Oral Surg Oral Med Oral Pathol* **78**, 522-530.
- [69] Love RM (2001) *Enterococcus faecalis*-A mechanism for its role in endodontic failure. *Int Endod* **34**, 399-405.
- [70] Takemura N, Noiri Y, Ehara A, Kawahara T, Noguchi N, Ebisu S (2004) Single-species biofilm-forming ability of root canal isolates on gutta-percha points. *Eur J Oral Sci* **112**, 523-529.
- [71] Wang J, Jiang Y, Chen W, Zhu C, Liang J (2012) Bacterial flora and extraradicular biofilm associated with the apical segment of teeth with post-treatment apical periodontitis. *J Endod* **38**, 954-959.

- [72] Walker JT, Dickinson J, Sutton JM, Raven ND, Marsh PD (2007) Cleanability of dental instruments—implications of residual protein and risks from Creutzfeldt-Jakob disease. *Br Dent J* **203**, 395-401.
- [73] Sonntag D, Peters OA (2007) Effect of prion decontamination protocols on nickel-titanium rotary surfaces. *J Endod* **33**, 442-446.
- [74] WHO/CDS/CSR/APH/2000, Centers for Disease Control and Prevention (2003) Guidelines for Infection Control in Dental Health-Care Settings. *MMWR Morb Mortal Wky Rep* **52**, 2003.
- [75] WHO consultation (1999) WHO Infection Control Guidelines for Transmissible Spongiform Encephalopathies. *World Health Organization Communicable Disease Surveillance and Control*, Geneva, Switzerland.
- [76] Azarpazhooh A, Fillery ED (2008) Prion disease: The implications for dentistry. *J Endod* **34**, 1158-1166.